**Engineering and Technology Journal e-ISSN: 2456-3358**
**Volume 07 Issue 07 July-2022, Page No.-1350-1361**
**DOI: 10.47191/etj/v7i7.05, I.F. – 6.484**


# A Study on Stability Analysis of 3-D Shear Deformable Isotropic Plate Elastically Restrained against Rotation and Simply Supported in the two Adjacent Edges using Exact Displacement Potential

**Onyeka, F. C.[1], Nwa-David, C. D.[2], Ikhazuagbe, Ohiwere.[3]**
[1]Department of Civil Engineering, Edo State University Uzairue, Edo State.
[2]Department of Civil Engineering, Michael Okpara University of Agriculture, Umudike.
[3]Department of Civil Engineering, Auchi Polytechnic, Auchi, Edo State, Nigeria

**ABSTRACT:** In this paper, a three-dimensional (3-D) stability analysis of rectangular deformable plate was performed to find the solution to the buckling problem of a uniaxially compressed plate in which the two adjacent loaded edges is clamped and the other, simply supported (CSCS). A three dimensional kinematics and constitutive relations were used to obtain the equation of total energy functional. The general and direct variation of the total potential energy function was done to get the general and direct governing equation of the plate by considering the effect of shear deformation. The solution of the general governing equation gave the deflection of the plate which is a product of the coefficient of deflection and shape function of the plate. The shape function is derived in terms of polynomial and trigonometric function and solved to get the exact deflection of the plate. The expression for the critical buckling load and other formulae was obtained by the direct variation of the total potential energy equation. This was done by minimizing the energy functional with respect to the coefficients of deflection after including the deflection and shear deformation rotation functions in it. The span to thickness ratio and aspect ratios were varied to ascertain the buckling behavior of different type of plate under uniformly distributed load. The outcome of the numerical analysis revealed that increase in the span-thickness ratio led to the increased value of the critical buckling load which implies that the plate structure is safe when the plate thickness is increased. The result showed that the critical buckling loads from the present study using polynomial are slightly higher than those obtained using trigonometric theories signifying the more exactness of the latter. The overall average percentage differences between the two functions recorded are 2.4%. This shows that at about 98% both approaches are the same and can be applied with confidence in the stability analysis of any type of plate with such boundary condition. The result of the present study using the established 3-D model for both functions is satisfactory and were found to follow an identical pattern, but quite distinct in validation which shows the credibility of the derived relationships.

**KEYWORDS**: CSCS rectangular plate, stability analysis 3-D plate, polynomial and trigonometric function, exact deflection potential.

## 1. INTRODUCTION

Plates are three-dimensional structural elements whose parallel plane surfaces are separated by a small dimension called “thickness”, and the relevance of plate materials in the construction industry and its application in marine, nuclear, mechanical, aerospace and structural engineering [1, 2]; is irrefutable. Based on the nature of the material and deformation properties, plates are categorized as orthotropic, anisotropic, and isotropic plates. Based on shapes, they can be triangular, circular plates or rectangular. As regards to their support conditions, plate edges can be simply supported, free or clamped [3]. Based on their depth or thickness, they can be classified as thin, moderately thick or thick plates [4]. Considering the span-depth ratio (a/t), rectangular plates with $50 \leq a/t \leq 100$ are classified as thin plate, $20 \leq a/t \leq 50$ as moderately thick and $a/t \leq 20$ as thick plate [5]. The unique properties of thick plates such as light weight, economy, ability to tailor the structural properties and its ability to withstand heavy loads [6], have attracted more research interest.

Based on the nature and kind of applied load, thick plates display dynamic, flexural and buckling behaviors [7]. Buckling is the commonest evidence of structural instability [8]. The phenomenon where a structure undergoes significant distortion and can no longer sustain its ability to withstand the load at a critical load value, is called buckling. Analyzing the stability of thick plates is of great importance as the interest for thick plates in the design of engineering structures have greatly increased.

Several researchers have considered different theories in order to avoid the rigorous nature of 3-D analysis by reducing the three-dimensional problem to two-dimensional by making an assumption that the strains can be expanded in the thickness dimension, integrating out the thickness dimension [9-12, 15-17]. Three-dimensional plate analysis is essential as two-dimensional analysis for a 3-D element often results to inaccurate and unreliable design.

Unlike the classical plate theory (CPT) formulated by Kirchhoff (1850) [9] which is mostly used for thin plate analysis, refined plate theory (RPT) addressed the transverse shear deformation effect. To account for the effect of shear deformation in the plate, the RPT which includes the first order shear deformation theory (FSDT) [10, 11], and second order shear deformation theory (SSDT) applied correction factor. In order to avoid the complication of a shear correction factor in plate analysis, higher order shear deformation theory (HSDT) was developed for a complete change in shear transverse stress on the plate surfaces [12, 13, 14]. However, RPT is an incomplete 3-D plate theory because of the neglected normal strain and stress along the thickness axis of the plate [15]. The use of 3-D plate theory is yet uncommon among recent researchers and a typical rectangular plate should be evaluated as a three-dimensional element. Applying equilibrium, numeric or energy methods [16], the stability of thick plates can also be analyzed.

Using work principle approach, Ibeabuchi *et al.* (2020) [17] examined the buckling of uniaxially compressed plate elastically restrained in all directions. The authors derived the buckling coefficients of the plate and developed a numerical model with polynomial displacement function. Their study was limited to CPT which can only be reliable in thin plate analysis. The 3-D plate theory was not applied and thick CSCS plates were not addressed.

Sayyad and Ghugal (2012) [18] employed RPT to analyze simply supported thick isotropic plates under biaxial and uniaxial in-plane forces using an assumed exponential function. They neither to take into account 3-D plate theory nor derive the displacement functional from the principle of elasticity. Also, their model did not account a CSCS plate's support condition.

Thick plates subjected to uniaxial in-plane compressive loading were investigated by Ezeh *et al.* (2018) [19]. The authors used an assumed polynomial displacement functions to analyze the buckling features of plates by considering Ritz principle. They could not apply 3-D plate theory with exact deflection functions and their study did not consider plate with the CSCS edge condition. Ibearugbulem *et al.* (2020) [20] used the same shape function and applied RPT to analyze the stability of thick plates. In their study, the strain energy and external work were combined to obtain the cumulative potential energy which was reduced to the governing equations. The authors obtained the critical load by substituting the polynomial function into the governing equation and the outcome was compared with those of FSDT. The authors [19 and 20] failed to consider plates with CSCS support conditions and also neglected all the stress and strain along the thickness direction of the plate. The exact displacement potential functional was also not derived.

Although Vareki *et al.* (2016) [21] applied displacement potential functions to solve the buckling problem of simply supported thick plates, they failed to employ exact displacement potential functional. Moslemi *et al.* (2016) [22] employed the same method (Love's displacement potential functions) to obtain exact solutions for the stability problem of thick plates of the same boundary condition. The authors solved two differential, partial equations of second and fourth orders to obtain the critical buckling load. The derived differential equations were analyzed using the method of variable separation. But they failed to consider CSCS (C: Clamped and S: Simply Supported edges) plates.

The stability of a 3-D simply supported rectangular thick plate (SSSS) and thick plate fixed at the supports (CCCC) under a compressive uniaxial load, were analyzed by Onyeka *et al.* (2022) [23 and 24] applying direct variational calculus with both polynomial-trigonometric displacement functions. Compared with the outcome of refined plate theories, their results were higher showing the exactness of their theory and the coarseness of the RPT. However, their study did not consider thick plates with the CSCS boundary condition. Onyeka *et al.* (2022) [25] employed a precise solution approach to develop a new model for analyzing the stability of three-dimensional plates CCFS support conditions. The authors obtained the true plates shape function from the equations of compatibility and the deflection coefficient of the plate from governing equation. Although the outcome of their 3-D model was satisfactory, they did not consider the application of exact displacement potential function for CSCS edge condition.

The buckling problem of a thick plate under uniform loading that was simply supported at the first and fourth edges, clamped and freely supported in the second and third edge respectively (SCFS), was analytically solved by Onyeka *et al.* (2022) [26]. The authors investigated the aspect ratio effect on the plate's critical buckling load without considering the use of exact trigonometric fuction. Also, the CSCS plate boundary condition was not debated.

The novelty of this study over the previous works lies in its method of analysis, plate theory, shape functions, and plate's edge conditions. The study is aimed at obtaining the buckling solution of a 3-D isotropic thick plate with two opposite edges clamped and simply supported (CSCS), using exact displacement potential functional. This work intends to achieve this through the following specific objectives by simplify the governing equations partial differential equations for the potential functions in form of polynomial

and trigonometric function thereafter the expressions for the critical buckling load of the plate was obtained using variational calculus.

## 2. THEORETICAL ANALYSIS

A three dimensional kinematics and constitutive relations was used to obtain the equation of total energy functional based on the static elastic theory of plate. The stress-strain relationship for an isotropic material under elastic condition as described using generalized Hooke's law is given as:

$$\begin{bmatrix} \varepsilon_x \\ \varepsilon_y \\ \varepsilon_z \\ \gamma_{xz} \\ \gamma_{yz} \\ \gamma_{xy} \end{bmatrix} = \frac{1}{E}\begin{bmatrix} 1 & -\mu & -\mu & 0 & 0 & 0 \\ -\mu & 1 & -\mu & 0 & 0 & 0 \\ -\mu & -\mu & 1 & 0 & 0 & 0 \\ 0 & 0 & 0 & 2(1+\mu) & 0 & 0 \\ 0 & 0 & 0 & 0 & 2(1+\mu) & 0 \\ 0 & 0 & 0 & 0 & 0 & 2(1+\mu) \end{bmatrix} \begin{bmatrix} \sigma_x \\ \sigma_y \\ \sigma_z \\ \tau_{xz} \\ \tau_{yz} \\ \tau_{xy} \end{bmatrix} \quad (1)$$

Where:

Modulus of elasticity and Poisson's ratios are denoted with E and μ respectively, the symbol $\varepsilon_x$ denotes normal strain along x axis, the symbol $\varepsilon_y$ denotes normal strain along y axis, the symbol $\varepsilon_z$ denotes normal strain along z axis, the symbol $\gamma_{xy}$ denotes shear strain in the plane parallel to the x-y plane, the symbol $\gamma_{xz}$ denotes shear strain in the plane parallel to the x-z plane, the symbol $\gamma_{yz}$ denotes shear strain in the plane parallel to the y-z plane.

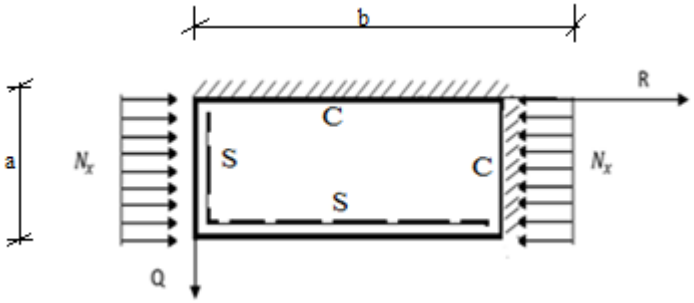


**Figure 1: CSCS Rectangular plate under uniaxial compressive load**

From the Figure 1, the non-dimensional form of coordinates is given as: R = x/a, Q = y/b and S = z/t corresponding to x, y and z-axes respectively. The spatial dimensions of the plate along x, y and z-axes are a, b and t respectively, as the t is the thickness of the plate, thus the six strain components is obtained using the established Hookes law (see ) as:

$$\varepsilon_x = \frac{St}{a}\frac{d\theta_x}{dR} \quad (2)$$

$$\varepsilon_y = \frac{St}{a\beta}\frac{d\theta_y}{dQ} \quad (3)$$

$$\varepsilon_z = \frac{1}{t}\frac{dw}{dS} \quad (4)$$

$$\gamma_{xy} = \frac{St}{a\beta}\frac{d\theta_x}{dQ} + \frac{St}{a}\frac{d\theta_y}{dR} \quad (5)$$

$$\gamma_{xz} = \theta_x + \frac{1}{a}\frac{dw}{dR} \quad (6)$$

$$\gamma_{yz} = \theta_y + \frac{1}{a\beta}\frac{dw}{dQ} \quad (7)$$

Similarly the six stress components gives:

$$\sigma_x = \frac{Ets}{(1+\mu)(1-2\mu)a}\left[(1-\mu).\frac{\partial\theta_x}{\partial R} + \frac{\mu}{\beta}.\frac{\partial\theta_y}{\partial Q} + \frac{\mu a}{st^2}.\frac{\partial w}{\partial S}\right] \quad (8)$$

$$\sigma_y = \frac{Ets}{(1+\mu)(1-2\mu)a}\left[\mu.\frac{\partial\theta_x}{\partial R} + \frac{(1-\mu)}{\beta}.\frac{\partial\theta_y}{\partial Q} + \frac{\mu a}{st^2}.\frac{\partial w}{\partial S}\right] \quad (9)$$

$$\sigma_z = \frac{Ets}{(1+\mu)(1-2\mu)a}\left[\mu.\frac{\partial\theta_x}{\partial R} + \frac{\mu}{\beta}.\frac{\partial\theta_y}{\partial Q} + \frac{(1-\mu)a}{st^2}.\frac{\partial w}{\partial S}\right] \quad (10)$$

$$\tau_{xy} = \frac{E(1-2\mu)ts}{2(1+\mu)(1-2\mu)a}.\left[\frac{1}{\beta}\frac{\partial\theta_x}{\partial Q} + \frac{\partial\theta_y}{\partial R}\right] \quad (11)$$

$$\tau_{xz} = \frac{E(1-2\mu)ts}{2(1+\mu)(1-2\mu)a}.\left[\frac{a}{ts}\theta_x + \frac{1}{ts}\frac{\partial w}{\partial R}\right] \quad (12)$$

$$\tau_{yz} = \frac{E(1-2\mu)ts}{2(1+\mu)(1-2\mu)a}.\left[\frac{a}{ts}\theta_y + \frac{1}{\beta ts}\frac{\partial w}{\partial Q}\right] \quad (13)$$

### 2.1. Energy Equation

Total potential energy functional is the algebraic summation of strain energy and external work. This mathematically expressed as:

$\prod = U - V$

Given that the strain energy is;

$$U = \frac{abt}{2}\int_0^1\int_0^1\int_{-0.5}^{0.5}\left(\sigma_x\varepsilon_x + \sigma_y\varepsilon_y + \sigma_z\varepsilon_z + \tau_{xy}\gamma_{xy} + \tau_{xz}\gamma_{xz} + \tau_{yz}\gamma_{yz}\right) dR\, dQ\, dS \quad (15)$$

And the external work for buckling load is given as:

$$V = \frac{abN_x}{2a^2}\int_0^a\int_0^b\left(\frac{\partial w}{\partial R}\right)^2 dR\, dQ \quad (16)$$

Putting Equations 2 to 13 into 15 and substituting 15 and 16 into 14 gives:

$$\Pi = D^*\frac{(1-\mu)ab}{2a^2(1-2\mu)}\int_0^1\int_0^1\left[(1-\mu)\left(\frac{\partial\theta_{sx}}{\partial R}\right)^2 + \frac{1}{\beta}\frac{\partial\theta_{sx}}{\partial R}\cdot\frac{\partial\theta_{sy}}{\partial Q} + \frac{(1-\mu)}{\beta^2}\left(\frac{\partial\theta_{sy}}{\partial Q}\right)^2 + \frac{(1-2\mu)}{2\beta^2}\left(\frac{\partial\theta_{sx}}{\partial Q}\right)^2 + \frac{(1-2\mu)}{2}\left(\frac{\partial\theta_{sy}}{\partial R}\right)^2 + \frac{6(1-2\mu)}{t^2}\left(a^2{\theta_{sx}}^2 + a^2{\theta_{sy}}^2 + \left(\frac{\partial w}{\partial R}\right)^2 + \frac{1}{\beta^2}\left(\frac{\partial w}{\partial Q}\right)^2 + 2a.\theta_{sx}\frac{\partial w}{\partial R} + \frac{2a.\theta_{sy}}{\beta}\frac{\partial w}{\partial Q}\right) + \frac{(1-\mu)a^2}{t^4}\left(\frac{\partial w}{\partial S}\right)^2 - \frac{N_x}{D^*}\cdot\left(\frac{\partial w}{\partial R}\right)^2\right]\partial R\partial Q \quad (17)$$

given that $D^*$ is the Rigidity for 3-D thick plate, let

$$D^* = D\,\frac{(1-\mu)}{(1-2\mu)}$$

where $D$ is the Rigidity of the CPT or incomplete 3-D thick plate, let

$N_x, \mu, w, \theta_{Sx}$, and $\theta_{Sy}$ are the uniform applied uniaxial compression load of the plate, the poison ratio, deflection , shear deformation rotation along x axis and shear deformation rotation along y axis respectively.

**2.2. Equilibrium and Governing Equation**

Minimizing the Energy equation (Equation 17) with respect to rotation in x-z plane and rotation in y-z plane $(\theta_{Sx}$, and $\theta_{Sy})$ and simplifying the outcome using the law of addition gives the two equations of equilibrium (Equations 18 and 19) in x-z plane and y-z plane respectively:

$$\frac{\partial w}{\partial R}\left[(1-\mu)\frac{\partial^2}{\partial R^2} + \frac{1}{\beta^2}\cdot\frac{\partial^2}{\partial Q^2}(1-\mu) + \frac{6(1-2\mu)a^2}{t^2}\cdot\left(1+\frac{1}{c}\right)\right] = 0 \quad (18)$$

$$\frac{1}{\beta}\cdot\frac{\partial w}{\partial Q}\left[\frac{\partial^2}{\partial R^2}(1-\mu) + \frac{(1-\mu)}{\beta^2}\frac{\partial^2}{\partial Q^2} + \frac{6(1-2\mu)a^2}{t^2}\cdot\left(1+\frac{1}{c}\right)\right] = 0 \quad (19)$$

One of the possibilities of Equation 18 to be true is for the terms in the bracket to sum to zero. Adding terms in the brackets of Equation 18 and 19 gives:

$$\frac{6(1-2\mu)(1+c)}{t^2} = -\frac{c(1-\mu)}{a^2}\left(\frac{\partial^2}{\partial R^2} + \frac{1}{\beta^2}\frac{\partial^2}{\partial Q^2}\right) \quad (20)$$

Similarly, the general governing equation is obtained by differentiating the Energy equation with respect to deflection and simplifying the outcome by substituting Equation 20 into it to get:

$$\frac{D^*}{2a^2}\int_0^1\int_0^1\left[\frac{6(1-2\mu)(1+c)}{t^2}\left(\frac{\partial^2 w}{\partial R^2} + \frac{1}{\beta^2}\cdot\frac{\partial^2 w}{\partial Q^2}\right) + \frac{(1-\mu)a^2}{t^4}\frac{\partial^2 w}{\partial S^2} - \frac{N_x}{D^*}\cdot\frac{\partial^2 w}{\partial R^2}\right] dR\, dQ = 0 \;\; 37$$

That is:

$$\frac{D^*}{2a^4}\int_0^1\int_0^1\left[\left(\frac{\partial^4 w_1}{\partial R^4} + \frac{2}{\beta^2}\cdot\frac{\partial^4 w_1}{\partial R^2\partial Q^2} + \frac{1}{\beta^4}\cdot\frac{\partial^4 w_1}{\partial Q^4} - \frac{N_{x1}a^4}{gD^*}\cdot\frac{\partial^2 w_1}{\partial R^2}\right)w_S + \frac{w_1}{g}\left(\frac{(1-\mu)a^4}{t^4}\cdot\frac{\partial^2 w_S}{\partial S^2} - \frac{N_{xs}a^4}{D^*}\cdot\frac{\partial^2 w_S}{\partial R^2}\right)\right] dR\, dQ = 0 \quad (21)$$

Where:

$$w = w_R.w_Q.w_S \quad (22)$$

$$w_1 = w_R.w_Q \quad (23)$$

$$N_x = N_{x1} + N_{xs} \quad (24)$$

For Equation 21 to be true, its integrand must be zero. That is:

$$\left(\frac{\partial^4 w_1}{\partial R^4} + \frac{2}{\beta^2}\cdot\frac{\partial^4 w_1}{\partial R^2\partial Q^2} + \frac{1}{\beta^4}\cdot\frac{\partial^4 w_1}{\partial Q^4} - \frac{N_{x1}a^4}{gD^*}\cdot\frac{\partial^2 w_1}{\partial R^2}\right)w_S + \frac{w_1}{g}\left(\frac{(1-\mu)a^4}{t^4}\cdot\frac{\partial^2 w_S}{\partial S^2} - \frac{N_{xs}a^4}{D^*}\cdot\frac{\partial^2 w_S}{\partial R^2}\right) \quad (25)$$

One of the possibilities of Equation 25 to be true is for the terms in each of the two brackets sum to zero. That is:

$$\frac{\partial^4 w_1}{\partial R^4} + \frac{2}{\beta^2}\cdot\frac{\partial^4 w_1}{\partial R^2\partial Q^2} + \frac{1}{\beta^4}\cdot\frac{\partial^4 w_1}{\partial Q^4} - \frac{N_{x1}a^4}{gD^*}\cdot\frac{\partial^2 w_1}{\partial R^2} = 0 \quad (26)$$

$$\frac{(1-\mu)a^4}{t^4}\cdot\frac{\partial^2 w_S}{\partial S^2} - \frac{N_{xs}a^4}{D^*}\cdot\frac{\partial^2 w_S}{\partial R^2} = 0 \quad (27)$$

Given that;

$$w = \mathrm{w}_1 . \mathrm{w}_S \quad (28)$$

Putting the Equation 28 into 26 and solve to get the exact deflection function in polynomial and trigonometric form as given in the Equation 29 and 30 respectively:

$$\mathrm{w} = \Delta_0 \,(a_0 + \ a_1 R + a_2 R^2 + a_3 R^3 + \ a_4 R^4).(b_0 + \ b_1 Q + \ b_2 Q^2 + b_3 Q^3 + b_4 Q^4) \quad (29)$$

$$w = \Delta_0 (a_0 + \ a_1 R + a_2 \cos g_1 R + a_3 \sin g_1 R).(b_0 + \ b_1 Q + b_2 \cos g_2 Q + b_3 \sin g_2 Q) \quad (30)$$

Where:

$$\mathrm{w} = A_1 . h \quad (31)$$

$$\mathrm{w}_S = \Delta_0 + \Delta_1 \mathrm{S} \quad (32)$$

And,

$$\mathrm{w}_S = \Delta_0 \quad (33)$$

Substituting Equation 29 and 30 into the re-arranged Equation 6 and simplifying the outcome gives:

$$\theta_{sx} = \frac{c}{a}.\Delta_0.(1 \ \ 2R \ \ 3R^2 \ \ 4R^3)\begin{bmatrix} a_1 \\ a_2 \\ a_3 \\ a_4 \end{bmatrix}.(1 \ \ Q \ \ Q^2 \ \ Q^3 \ \ Q^4)\begin{bmatrix} b_0 \\ b_1 \\ b_2 \\ b_3 \\ b_4 \end{bmatrix} \quad (34)$$

$$\theta_{Sx} = \frac{c}{a}.\Delta_0.[1 \ \ c_1 Sin\,(c_1 R) \ \ c_1 Cos\,(c_1 R)]\begin{bmatrix} a_1 \\ a_2 \\ a_3 \end{bmatrix}.[1 \ \ Q \ \ Cos\,(c_1 Q) \ \ Sin\,(c_1 Q)]\begin{bmatrix} b_0 \\ b_1 \\ b_2 \\ b_3 \end{bmatrix} \quad (35)$$

Similarly;

$$\theta_{sy} = \frac{c}{a\beta}.\Delta_0.(1 \ \ R \ \ R^2 \ \ R^3 \ \ R^4)\begin{bmatrix} a_0 \\ a_1 \\ a_2 \\ a_3 \\ a_4 \end{bmatrix}.(1 \ \ 2Q \ \ 3Q^2 \ \ 4Q^3)\begin{bmatrix} b_1 \\ b_2 \\ b_3 \\ b_4 \end{bmatrix} \quad (36)$$

$$\theta_{sy} = \frac{c}{a\beta}.\Delta_0.[1 \ \ R \ \ Cos\,(c_1 R) \ \ Sin\,(c_1 R)]\begin{bmatrix} a_0 \\ a_1 \\ a_2 \\ a_3 \end{bmatrix}.[1 \ \ c_1 Sin\,(c_1 Q) \ \ c_1 Cos\,(c_1 Q)]\begin{bmatrix} b_1 \\ b_2 \\ b_3 \end{bmatrix} \quad (37)$$

In symbolic forms, Equations 34 and 35 are:

$$\theta_{sx} = \frac{A_{2R}}{a}.\frac{\partial h}{\partial R} \quad (38)$$

While Equations 36 and 37 are:

$$\theta_{sy} = \frac{A_{2Q}}{a\beta}.\frac{\partial h}{\partial Q} \quad (39)$$

Given that;

Given that: $h$ is the shape function of the plate, $A_1$ is the coefficient of deflection $A_2$ and $A_3$ are the coefficients of shear deformation in x axis and y axis respectively.

Where:

The coefficient of deflection;

$$A_1 = \Delta_0 \begin{bmatrix} a_0 \\ a_1 \\ a_2 \\ a_3 \\ a_4 \end{bmatrix}.\begin{bmatrix} b_0 \\ b_1 \\ b_2 \\ b_3 \\ b_4 \end{bmatrix} \quad (40)$$

The trigonometric shape function;

$$h = (1 \ \ R \ \cos g_1 R \ \sin g_1 R).(1 \ Q \ \cos g_2 Q \ \sin g_2 Q) \quad (41)$$

The polynomial shape function;

$$h = [1 \ \ R \ R^2 \ R^3 \ \ R^4].[1 \ \ Q \ Q^2 \ Q^3 \ Q^4] \quad (42)$$

### 2.3. Direct Governing Equation

By substituting Equations (31), (38) and (39) into the Energy equation obtained in Equation (17) and differentiating with respect to deflection coefficient ($A_1$), the direct governing equation of the plate is given as:

$$\frac{\partial \Pi}{\partial A_1} = 6(1-2\mu)\left(\frac{\mathrm{a}}{t}\right)^2\left([A_1 + M_2 A_1].k_R + \frac{1}{\beta^2}.[A_1 + M_3 A_1].k_Q\right) - \frac{\mathrm{N_x a^2} A_1}{\mathrm{D^*}}.k_R = 0 \quad (43)$$

Rearranging Equation 43 gives:

$$\frac{\mathrm{N_x a^2}}{\mathrm{D^*}} = 6(1-2\mu)\left(\frac{\mathrm{a}}{t}\right)^2\left([1 + M_2] + \frac{1}{\beta^2}.[1 + M_3].\frac{k_Q}{k_R}\right) \quad (44)$$

This gives:

$$\frac{\mathrm{a^2 N_x}}{Et^3} = \frac{(1+\mu)}{2}\left(\frac{\mathrm{a}}{t}\right)^2\left([1 + M_2] + \frac{1}{\beta^2}.[1 + M_3].\frac{k_Q}{k_R}\right) \quad (45)$$

Where:

$$k_{RR} = \int_0^1 \int_0^1 \left(\frac{\partial^2 h}{\partial R^2}\right)^2 dRdQ;\ k_{RQ} = \int_0^1 \int_0^1 \left(\frac{\partial^2 h}{\partial R \partial Q}\right)^2 dRdQ;\ k_{QQ} = \int_0^1 \int_0^1 \left(\frac{\partial^2 h}{\partial Q^2}\right)^2 dRdQ \quad (45a)$$

$$k_R = \int_0^1 \int_0^1 \left(\frac{\partial h}{\partial R}\right)^2 dRdQ;\ k_Q = \int_0^1 \int_0^1 \left(\frac{\partial h}{\partial Q}\right)^2 dRdQ \quad (45b)$$

Minimizing Equation 54 with respect to $A_{2R}$ and $A_{2Q}$ and Solving Equations simultaneously gives respectively:

$$A_{2R} = M_2 A_1 \quad (46)$$

$$A_{2Q} = M_3 A_1 \quad (47)$$

Where:

$$M_2 = \frac{(m_{12}m_{23} - m_{13}m_{22})}{(m_{12}m_{12} - m_{11}c_{22})};\ M_3 = \frac{(m_{12}m_{13} - m_{11}m_{23})}{(m_{12}m_{12} - m_{11}m_{22})} \quad (48)$$

$$m_{11} = (1-\mu)k_{RR} + \frac{1}{2\beta^2}(1-2\mu)k_{RQ} + 6(1 - 2\mu)\left(\frac{a}{t}\right)^2 k_R \quad (49)$$

$$m_{22} = \frac{(1-\mu)}{\beta^4}k_{QQ} + \frac{1}{2\beta^2}(1-2\mu)k_{RQ} + \frac{6}{\beta^2}(1-2\mu)\left(\frac{a}{t}\right)^2 k_Q \quad (50)$$

$$m_{12} = m_{21} = \frac{1}{2\beta^2}k_{RQ};\ m_{13} = -6(1-2\mu)\left(\frac{a}{t}\right)^2 k_R;\ m_{23} = m_{32} = -\frac{6}{\beta^2}(1-2\mu)\left(\frac{a}{t}\right)^2 k_Q \quad (51)$$

**2.4. Numerical Analysis**

A problem of a rectangular thick plate that is clamped at two adjacent edges and the other simply supported (CSCS) under uniaxial compressive load is presented. The polynomial and trigonometric displacement function as presented in the Equation (29) and (30) was applied to obtain the solution of the critical buckling load in the plate at various aspect ratios. The boundary conditions of the rectangular plate presented in the Figure 1 are as follows:

At $R = Q = 0$; deflection $(w) = 0$ (52)

At $R = 0$, bending moment $\left(\frac{d^2w}{dR^2}\right) = 0;\ Q = 0$, slope $\left(\frac{dw}{dQ}\right) = 0$ (53)

At $R = Q = 1$, deflection $(w) = 0$; (54)

At $R = 1$, bending moment $\left(\frac{d^2w}{dR^2}\right) = 0;\ Q = 1$, shear force $\left(\frac{d^3w}{dQ^3}\right) = 0$ (55)

At $Q = 1$, bending moment $\left(\frac{d^2w}{dR^2}\right) = 0;\ R = 1$, slope $\left(\frac{dw}{dQ}\right) = 0$ (56)

Substituting Equation (52) to (56) into the derivatives of w and solving gave the characteristic equation gives the following constants:

$$a_0 = 0;\ a_1 = a_4;\ a_2 = 0;\ a_3 = -2a_4\ and \quad (57)$$

$$b_0 = 0;\ b_1 = 0;\ b_2 = 2b_4;\ b_3 = -2b_4 \quad (58)$$

Substituting the constants of Equation (57) and (58) into Equation (29) gives;

$$w = (a_4R - a_4R^3 + a_4R^4) \times (b_4Q^2 - b_4Q^3 + b_4Q^4) \quad (59)$$

Simplifying Equation (59) which satisfying the boundary conditions of Equation (52 to 56) gives:

$$w = a_4 \times b_4(R - 2R^3 + R^4) \times (Q^2 - 2Q^3 + Q^4) \quad (60)$$

Let the amplitude,

$$A_1 = a_4 \times b_4$$

And;

$$h = (R - 2R^3 + R^4) \times (Q^2 - 2Q^3 + Q^4) \quad (62)$$

Thus, the polynomial deflection functions after satisfying the boundary conditions is:

$$w = (R - 2R^3 + R^4) \times (Q^2 - 2Q^3 + Q^4).A_1 \quad (63)$$

Similarly, substituting Equations (52 to 56) into Equation (30) and solving gives the following constants:

$$sing_1 = 0;\ 2Cos\ g_1 + g_1\ Sin\ g_1 - 2 = 0 \quad (64)$$

The value of $g_1$ that satisfies Equation (64) is:

$g_1 = m\pi\ ; g_1 = 2m\pi\ [where\ m = n = 1, 2, 3 \ldots]$ (65)

Substituting Equation (65) into the derivatives of w and satisfying the boundary conditions of Equation (52) to (56) gives the following constants:

$a_0 = a_1 = a_2;\ \ b_1 = b_3 = 0;\ b_0 = -b_2 = 0$ (66)

Substituting the constants of Equation (66) into Equation (30) and simplify the outcome gives:

$w = a_3 \times b_2 (Sin\ \pi R).(Cos\ 2\pi Q - 1)$ (67)

Let the amplitude,

$A_1 = a_3 \times b_2$ (68)

And;

$h = (Sin\ \pi R).(Cos\ 2\pi Q - 1)$ (69)

Thus, the trigonometric deflection functions after satisfying the boundary conditions is:

$w = A_1 (Sin\ \pi R).(Cos\ 2\pi Q - 1)$ (70)

As such, a numerical values of the stiffness for a CSCS plate were obtained using Equation (45a) and (45b) by applying the two shape function (trigonometric and polynomial) as obtained in Equation (62) and Equation (69) and their results are presented in Table 1.

**Table 1. The polynomial and trigonometric stiffness coefficients of deflection function of the CSFS plate**

| Displacement Shape Function | $k_{RR}$ | $k_{RQ}$ | $k_{QQ}$ | $k_R$ | $k_Q$ |
|---|---|---|---|---|---|
| Polynomial | 0.00762 | 0.00925 | 0.03937 | 0.00077 | 0.00925 |
| Trigonometry | $\frac{3\pi^4}{4}$ | $\pi^4$ | $4\pi^4$ | $\frac{3\pi^2}{4}$ | $\pi^2$ |

## 3. RESULTS AND DISCUSSIONS

In this section, Equation (29) and (30) showed the expression of deflection function which was derived to get the formulae for predicting the buckling load of the plate. The graphical re-presentation of the result of the critical buckling load of a rectangular plate that is clamped and simply supported at the two adjacent edges (CSCS), as calculated is shown in the Figures 2 to 10. This result also showed the comparative stability analysis of the CSCS plate under uniaxial compressive load at varying aspect ratio. The first non-dimensional result was obtained by expressing the displacement shape function of the plate in the form of polynomial to analyze the effect of aspect ratio on the critical buckling load of the plate while the second result was obtained by expressing the displacement shape function of the plate in the form of trigonometry to analyze the effect of aspect ratio on the critical buckling load of the plate. The aspect ratio of the plate into consideration includes; 1, 1.5, 2.0, 2.5, 3.0, 3.5, 4.0, 4.5 and 5.0. A numerical and graphical comparison was made between the two approaches (polynomial and trigonometric functions) to study a 3-D plate's stability at varying thickness. The span to thickness ratio considered is ranged between 4 through 1500, which is obviously seen to span from the thick plate, moderately thick plate and thin plate (see [2 and 12]).

The values obtained in Figure 2 to 10, shows that as the values of critical buckling load increase, the span- thickness ratio increases. This reveals that as the in-plane load on the plate increase and approaches the critical buckling, the failure in a plate structure is a bound to occur; this means that a decrease in the thickness of the plate, increases the chance of failure in a plate structure. Hence, failure tendency in the plate structure can be mitigated by increasing its thickness. It is also observed in the figures that as the length to breadth ratio (aspect ratio) of the plate increases, the value of critical buckling load decreases while as critical buckling load increases as the length to breadth ratio increases. This implies that an increase in plate width increases the chance of failure in a plate structure. It can be deduced that as the in-plane load which will cause the plate to fail by compression increases from zero to critical buckling load, the buckling of the plate exceeds specified elastic limit thereby causing failure in the plate structure. This meant that, the load that causes the plate to deform also causes the plate material to buckle simultaneously.

Looking closely at the result of buckling load using Polynomial function for the span to thickness ratio of 30 and beyond, it is seen that the value of critical buckling load of the plate maintained a constant value of 8.49 for square plate, 3.06 for aspect ratio of 1.5, 1.90 for aspect ratio of 2.0, 1.50 for aspect ratio of 2.5, 1.32 for aspect ratio of 3.0, 1.22 for aspect ratio of 3.5, 1.16 for aspect ratio of 4.0, 1.12 for aspect ratio of 4.5, 1.09 for aspect ratio of 5.0. Similarly, the result of buckling load using Trigonometric function for the span to thickness ratio of 30 and beyond, it is seen that the value of critical buckling load of the plate maintained a constant value

of 8.84 for square plate, 3.19 for aspect ratio of 1.5, 1.97 for aspect ratio of 2.0, 1.54 for aspect ratio of 2.5, 1.34 for aspect ratio of 3.0, 1.24 for aspect ratio of 3.5, 1.17 for aspect ratio of 4.0, 1.13 for aspect ratio of 4.5, 1.10 for aspect ratio of 5.0. This proof that the value of critical load for thin plate and thick plate (see [2 and 12]) which described the thin and moderately thick plate as the one whose span to thickness ratio is equal or less than 30.

The comparison shows that the present theory using trigonometric functions predicts a slightly lower value of the critical buckling load than polynomial function when the plate is thicker and higher value as the plate is thinner. This is quite expected because the trigonometric function gives higher value of the stiffness coefficient than polynomial, and therefore is considered safer to use for thick plate analysis. However, both functions provide exact solution using 3-D theory in the stability analysis of a rectangular plate. The percentage difference of critical buckling load between the present study using polynomial, and that of trigonometric function for an isotropic CSCS rectangular plate at a variable aspect ratio is presented in Table. The highest average percentage difference is 7.4295 which occurs at the square plate using polynomial function, while the lowest average percentage difference is 0.9461 which occur in an aspect ratio of five (5) using trigonometric function. It is shown in the table that the degree of the error in percentage decreases as the aspect ratio of the plate decreases. This implies that as the length of the plate widens, the credibility of the two approaches (trigonometry and polynomial) becomes the same. Furthermore, it was discovered that the values of the percentage error decrease as the span to thickness ratio of the plate decrease for the two approaches in consideration. This implies that as the plate gets thinner, the two methods differs more and becomes almost the same for thick plates. This could mean that the two approaches are suitable for thick plate analysis. This, however, shows the high level of convergence between the two approaches. It also implies a high level of accuracy of the derived relationships and thus proof reliability of the process in the stability analysis of rectangular plate of any category (thin, moderately thick and thick plate). Finally, the overall average percentage differences between the two functions recorded are 2.4%. These differences being less than 5% are quite acceptable in statistical analysis, as it will not put the structure into danger [3]. This shows that at about 98% both approaches are the same and can be applied with confidence in the stability analysis of any type of plate with such boundary condition.

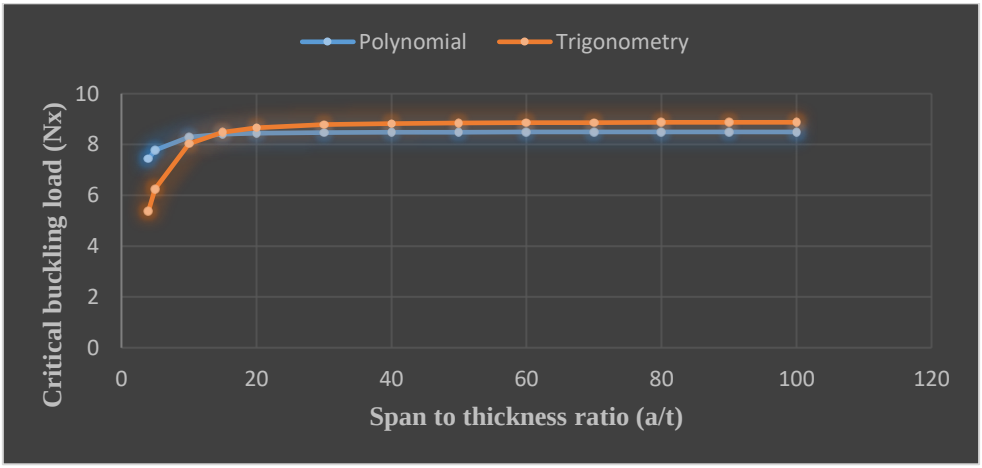


**Figure 2. Graph of Critical buckling load ($N_x$) versus span to thickness ratio of a rectangular plate at aspect ratio of 1.0**

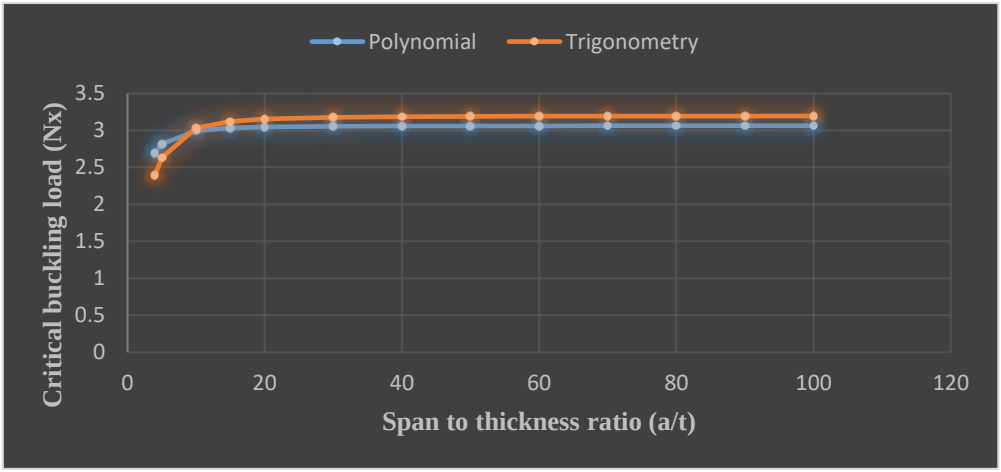


**Figure 3. Graph of Critical buckling load ($N_x$) versus span to thickness ratio of a rectangular plate at aspect ratio of 1.5**

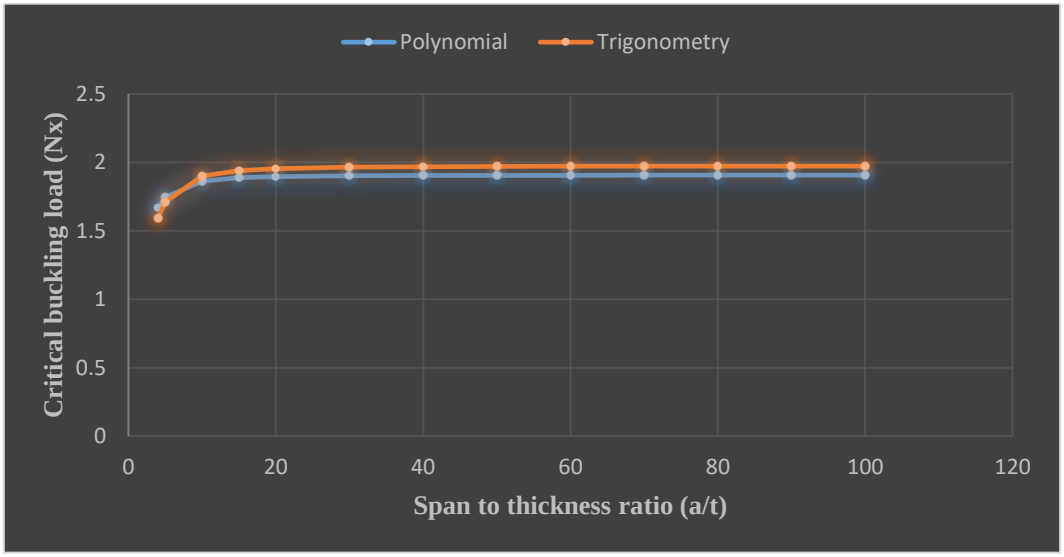


**Figure 4. Graph of Critical buckling load ($N_x$) versus span to thickness ratio of a rectangular plate at aspect ratio of 2.0**

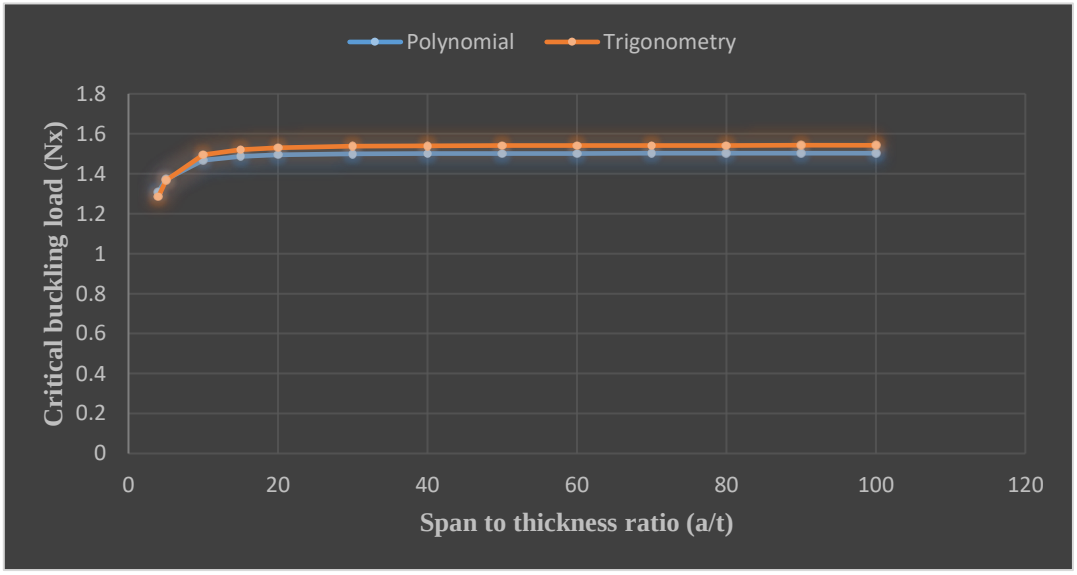


**Figure 5. Graph of Critical buckling load ($N_x$) versus span to thickness ratio of a rectangular plate at aspect ratio of 2.5**

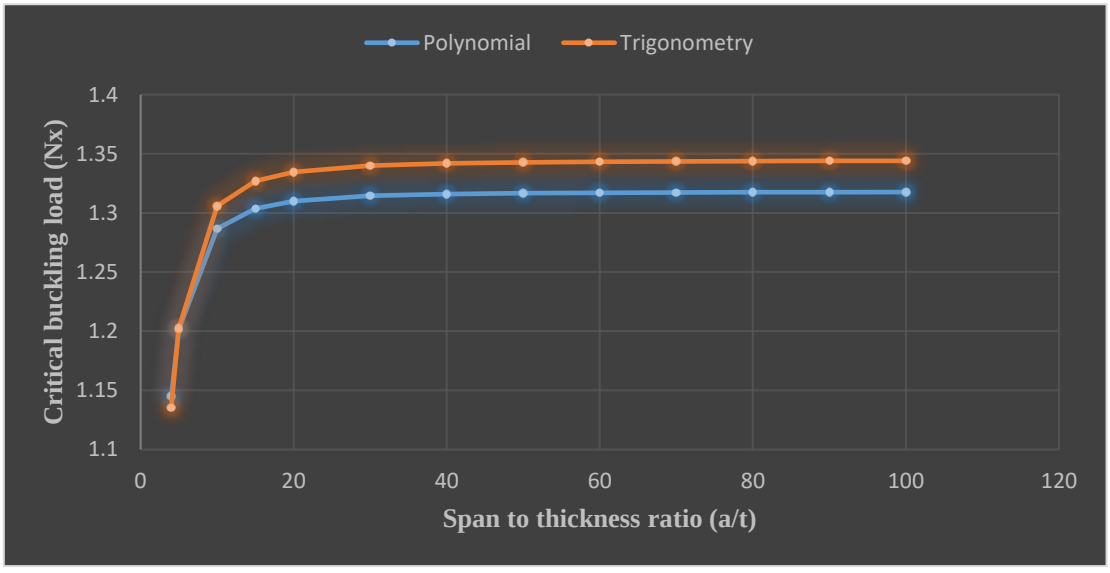


**Figure 6. Graph of Critical buckling load ($N_x$) versus span to thickness ratio of a rectangular plate at aspect ratio of 3.0**

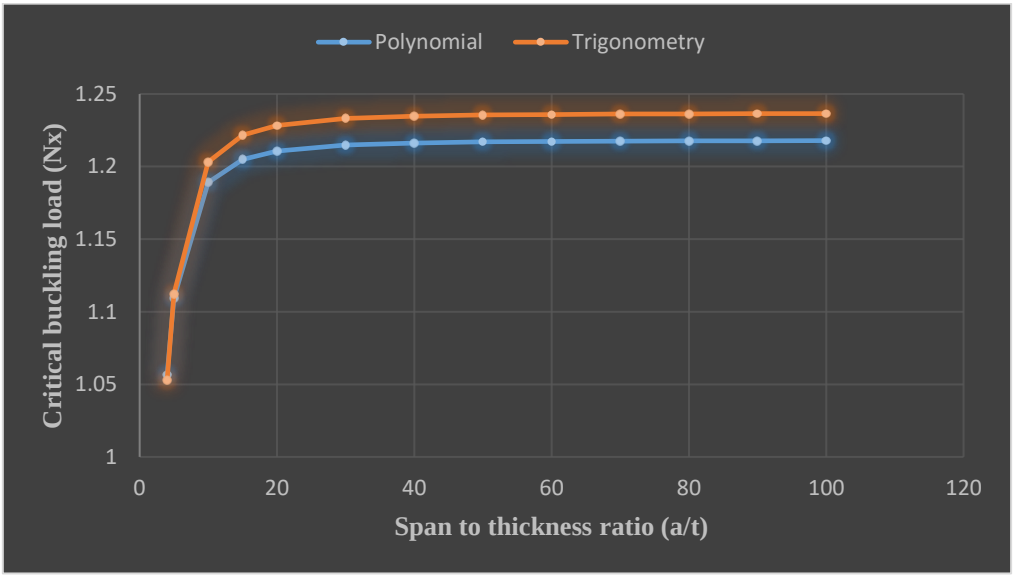


**Figure 7. Graph of Critical buckling load ($N_x$) versus span to thickness ratio of a rectangular plate at aspect ratio of 3.5**

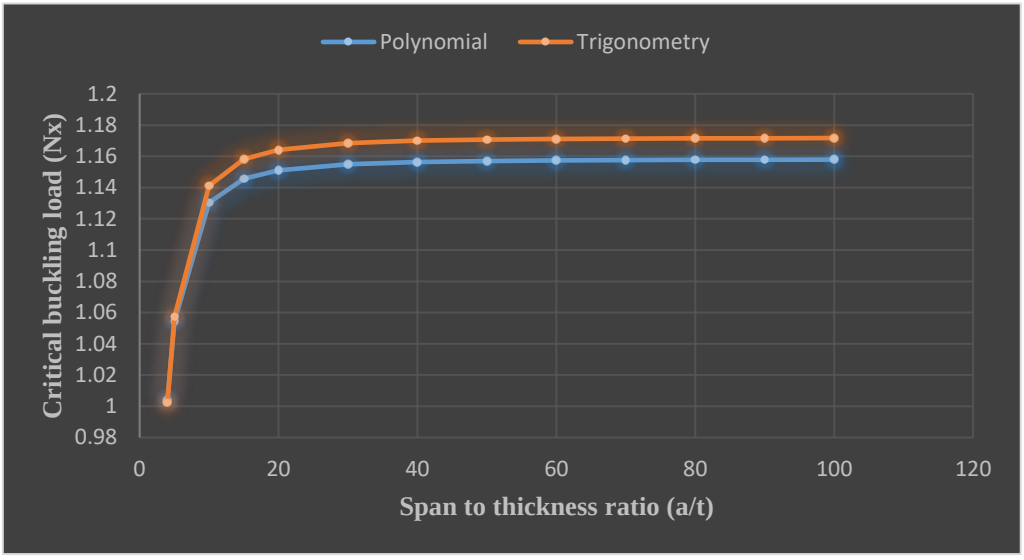


**Figure 8. Graph of Critical buckling load ($N_x$) versus span to thickness ratio of a rectangular plate at aspect ratio of 4.0**

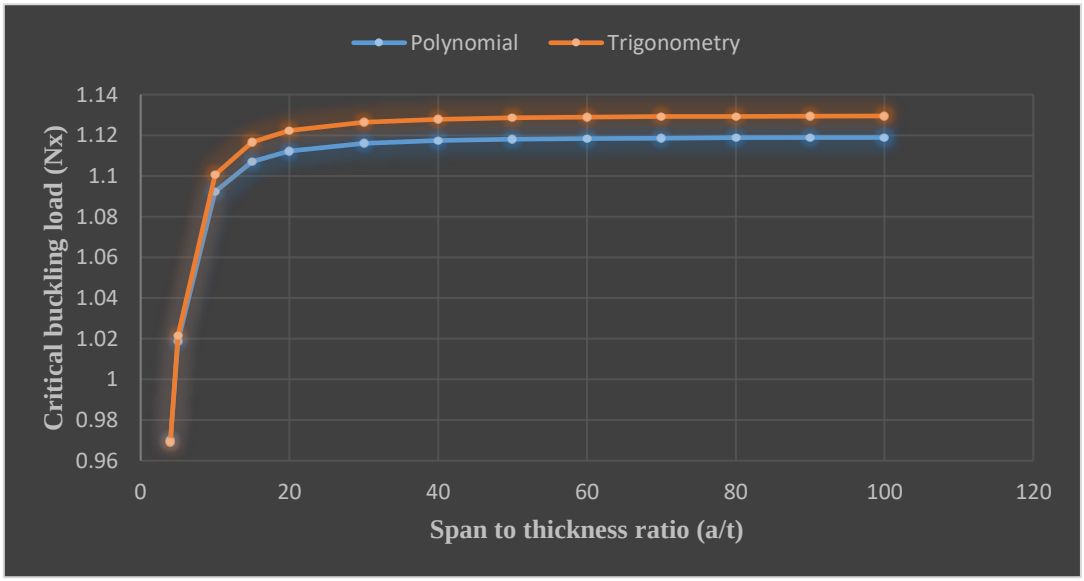


**Figure 9. Graph of Critical buckling load ($N_x$) versus span to thickness ratio of a rectangular plate at aspect ratio of 4.5**

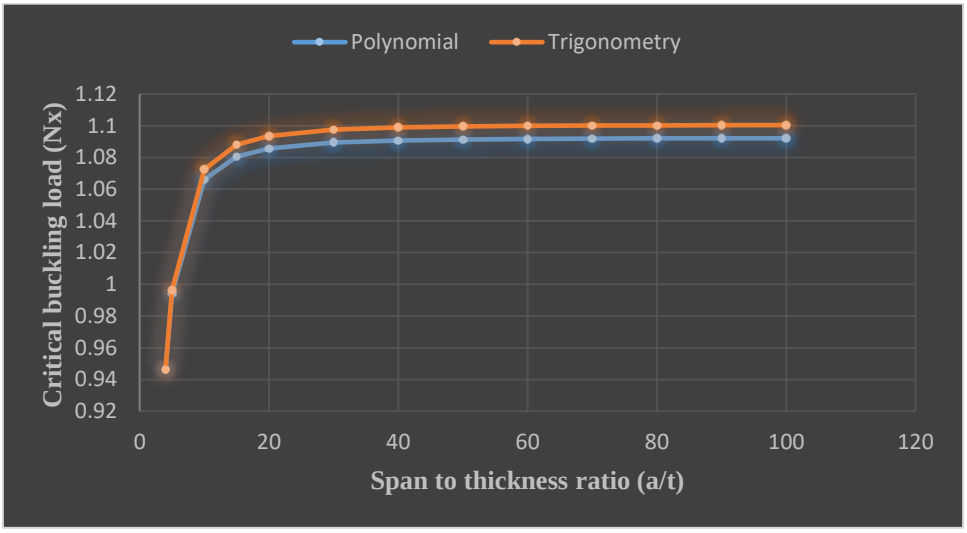


**Figure 10. Graph of Critical buckling load ($N_x$) versus span to thickness ratio of a rectangular plate at aspect ratio of 5.0**

## 4. CONCLUSION AND RECOMMENDATION

The result of this study as recorded in the percentage difference analysis showed that the 2-D refined plate theory (RPT) is only an approximate relation for buckling analysis of thick plate [22] and when applied to the thick plate will under-predicts buckling loads as they neglect the transverse normal stresses along the thickness axis of the plate. Thus, the polynomial and trigonometric displacement function developed in this study produces an exact solution as they emanated from a complete three-dimensional theory which is more reliable solution in the stability analysis of plates and, can be recommended for analysis of any type of rectangular plate subjected to such loading and boundary condition.

## REFERENCES


1. F. C. Onyeka, "Critical Lateral Load Analysis of Rectangular Plate Considering Shear Deformation Effect," *Global Journal of Civil Engineering*, vol. 1, pp. 16-27, 2020. doi: 10.37516/global.j.civ.eng.2020.012
2. F.C. Onyeka., C.D. Nwa-David, and E.E. Arinze, "Structural Imposed Load Analysis of Isotropic Rectangular Plate Carrying a Uniformly Distributed Load Using Refined Shear Plate Theory", *FUOYE Journal of Engineering and Technology (FUOYEJET)*, 6(4), 414-419, 2021. http://dx.doi.org/10.46792/fuoyejet.v6i4.719
3. J. N. Reddy, "Classical Theory of Plates. In Theory and Analysis of Elastic Plates and Shells", CRC Press. 2006. doi:10.1201/9780849384165-7.
4. K. Chandrashekhara, "Theory of plates". *University Press (India) Limited*. 2000.
5. F. C. Onyeka, and T. E. Okeke, "New refined shear deformation theory effect on non-linear analysis of a thick plate using energy method," *Arid Zone Journal of Engineering, Technology and Environment*, vol. 17, no. 2, pp. 121-140, 2021.
6. F. C. Onyeka, T. E. Okeke, "Analysis of Critical Imposed Load of Plate Using Variational Calculus," *Journal of Advances in Science and Engineering*, vol. 4, no. 1, pp. 13–23, 2020. Doi: https://doi.org/10.37121/jase.v4i1.125
7. F. C. Onyeka, "Effect of Stress and Load Distribution Analysis on an Isotropic Rectangular Plate," *Arid Zone Journal of Engineering, Technology and Environment*, vol. 17, no. 1, pp. 9-26, 2021.
8. F. C. Onyeka and D. Osegbowa, "Stress analysis of thick rectangular plate using higher order polynomial shear deformation theory. *FUTO Journal Series – FUTOJNLS*, vol. 6, no. 2, pp. 142-161, 2020.
9. F. C. Onyeka, B. O. Mama, C. D. Nwa-David, "Application of Variation Method in Three Dimensional Stability Analysis of Rectangular Plate Using Various Exact Shape Functions." *Nigerian Journal of Technology*, vol. 41, no. 1, pp. 8-20, 2022. doi: http://*dx.doi.org/10.4314/njt.v41i1.2*.
10. G R. Kirchhoff, "U''ber Das Gleichgewicht and Die Bewe Gung Einer Elastschen Scheibe". *Journal f'' Ur Die Reine Und Angewandte Mathematik* 40, 51–88, 1850. doi:10.1515/crll.1850.40.51.
11. E. Reissner, "The Effect of Transverse Shear Deformation on the Bending of Elastic Plates". *Journal of Applied Mechanics* 12, (2) A69–A77, 1945. doi:10.1115/1.4009435.
12. R. D Mindlin, "Influence of Rotatory Inertia and Shear on Flexural Motions of Isotropic, Elastic Plates". *Journal of Applied Mechanics* 18(1): 31–38. 1951. doi:10.1115/1.4010217.

13. F. C. Onyeka, F. O. Okafor, H. N. Onah, "Application of a New Trigonometric Theory in the Buckling Analysis of Three-Dimensional Thick Plate," *International Journal of Emerging Technologies*, vol. 12, no. 1, pp. 228-240, 2021.
14. F. C. Onyeka and T. E. Okeke, "Elastic Bending Analysis Exact Solution of Plate using Alternative I Refined Plate Theory*," Nigerian Journal of Technology (NIJOTECH),* vol. 40, no. 6, pp. 1018 – 1029, 2021. doi: http://dx.doi.org/10.4314/njt.v40i6.4.
15. F. C. Onyeka, and B. O. Mama, "Analytical Study of Bending Characteristics of an Elastic Rectangular Plate using Direct Variational Energy Approach with Trigonometric Function". *Emerging Science Journal.* 5, (6), 916-928, 2021. doi: http://dx.doi.org/10.28991/esj-2021-01320.
16. N. G. Iyengar, "Structural Stability of Columns and Plates." New York, Ellis Horwood Limited. 1988.
17. V.T. Ibeabuchi, O.M. Ibearugbulem, C. Ezeah, and O.O. Ugwu, "Elastic Buckling Analysis of Uniaxially Compressed CCCC Stiffened Isotropic Plates". *Int. J. of Applied Mechanics and Engineering*, *25*(4): 84-95, 2020.
18. A.S. Sayyad, and Y.M. Ghugal, "Buckling analysis of thick isotropic plates by using exponential shear deformation theory". *Journal of Applied and Computational Mechanics*, 6: 185 – 196, 2012.
19. J. C. Ezeh, I. C. Onyechere, O. M. Ibearugbulem, U. C. Anya, and L. Anyaogu "Buckling Analysis of Thick Rectangular Flat SSSS Plates using Polynomial Displacement Functions". *International Journal of Scientific & Engineering Research*. 9 (9), 387-392, 2018.
20. O. M. Ibearugbulem, S. I. Ebirim, U.C. Anya, L. O. Ettu "Application of Alternative II Theory to Vibration and Stability Analysis of Thick Rectangular Plates (Isotropic and Orthotropic)". *Nigerian Journal of Technology (NIJOTECH).* 39(1), 52-62, 2020. http://dx.doi.org/10.4314/njt.v39i1.6
21. A.M. Vareki, B.N. Neya, and J.V. Amiri, "3-D Elasticity Buckling Solution for Simply Supported Thick Rectangular Plates using Displacement Potential Functions". *Applied Mathematical Modelling*, *40,* 5717–5730, 2016. https://doi.org/10.1016/j.apm.2015.12.034
22. A. Moslemi, B. N. Neya, J. V. Amiri, "3-D elasticity buckling solution for simply supported thick rectangular plates using displacement potential functions". *Applied Mathematical Modelling* 40, 5717–5730, 2016. doi: http://dx.doi.org/10.1016/j.apm.2015.12.034.
23. F. C. Onyeka, B. O. Mama, T. E. Okeke, "Exact Three-Dimensional Stability Analysis of Plate Using Direct Variational Energy Method". *Civil Engineering Journal*. 8(1). 60-80, 2022. doi: http://dx.doi.org/10.28991/CEJ-2022-08-01-05.
24. F.C. Onyeka, F. O. Okafor, and H. N. Onah, "Buckling Solution of a Three-Dimensional Clamped Rectangular Thick Plate Using Direct Variational Method," *IOSR Journal of Mechanical and Civil Engineering (IOSR-JMCE*), 18(3), 10-22, 2021. doi: 10.9790/1684-1803031022.
25. F.C. Onyeka, B. O. Mama, and C. D. Nwa-David, "Analytical Modelling of a Three-Dimensional (3D) Rectangular Plate Using the Exact Solution Approach," *IOSR Journal of Mechanical and Civil Engineering (IOSR-JMCE),* 11(1), 10-22, 2022.doi: 10.9790/1684-1901017688.
26. F. C. Onyeka, B. O. Mama, J. Wasiu, "An Analytical 3-D Modeling Technique of Non-Linear Buckling Behavior of an Axially Compressed Rectangular Plate. *International Research Journal of Innovations in Engineering and Technology – IRJIET"* 6(1), 91-101, 2022. doi https://doi.org/10.47001/IRJIET/2022.601017.